LETTER

doi:10.1038/nature10234

Integrative genomics identifies MCU as an essential component of the mitochondrial calcium uniporter

Joshua M. Baughman[1,2]*, Fabiana Perocchi[1,2]*, Hany S. Girgis[1,2], Molly Plovanich[1,2], Casey A. Belcher-Timme[1,2], Yasemin Sancak[1,2], X. Robert Bao[1,2], Laura Strittmatter[1,2], Olga Goldberger[1,2], Roman L. Bogorad[3], Victor Koteliansky[4] & Vamsi K. Mootha[1,2]

Mitochondria from diverse organisms are capable of transporting large amounts of Ca^{2+} via a ruthenium-red-sensitive, membrane-potential-dependent mechanism called the uniporter[1–4]. Although the uniporter's biophysical properties have been studied extensively, its molecular composition remains elusive. We recently used comparative proteomics to identify MICU1 (also known as CBARA1), an EF-hand-containing protein that serves as a putative regulator of the uniporter[5]. Here, we use whole-genome phylogenetic profiling, genome-wide RNA co-expression analysis and organelle-wide protein coexpression analysis to predict proteins functionally related to *MICU1*. All three methods converge on a novel predicted transmembrane protein, CCDC109A, that we now call 'mitochondrial calcium uniporter' (MCU). MCU forms oligomers in the mitochondrial inner membrane, physically interacts with MICU1, and resides within a large molecular weight complex. Silencing *MCU* in cultured cells or *in vivo* in mouse liver severely abrogates mitochondrial Ca^{2+} uptake, whereas mitochondrial respiration and membrane potential remain fully intact. MCU has two predicted transmembrane helices, which are separated by a highly conserved linker facing the intermembrane space. Acidic residues in this linker are required for its full activity. However, an S259A point mutation retains function but confers resistance to Ru360, the most potent inhibitor of the uniporter. Our genomic, physiological, biochemical and pharmacological data firmly establish MCU as an essential component of the mitochondrial Ca^{2+} uniporter.

To predict proteins that are functionally related to MICU1 (ref. 5) and essential for mitochondrial calcium (Ca^{2+}) uptake, we performed three systematic computational analyses. First, we ranked all ~20,000 mammalian genes on the basis of the similarity of their phylogenetic profile to *MICU1*, where the phylogenetic profile of a gene is defined as the binary vector of presence or absence of its homologues across 500 evolutionarily diverse organisms[6,7]. Second, we scored all ~20,000 mammalian genes for their expression similarity to *MICU1* across 81 mouse cell types and tissues using a genome-wide RNA expression atlas[8]. Third, we scored protein expression similarity between MICU1 and all ~1,100 mitochondrial proteins, based on their pattern of peptide abundance across 14 different mouse tissues[6]. All three computational methods (Fig. 1a–c) spotlight an unstudied protein (previously called CCDC109A, accession number NM_138357.1) that we now call 'mitochondrial calcium uniporter' (MCU). MCU, which has two predicted transmembrane domains, was first discovered in our proteomic analysis as a mitochondrial protein detected in 12 different mouse tissues[6]. *MCU*, which bears no sequence similarity to *MICU1*, is tied as the eighth closest phylogenetic neighbour genome-wide (Fig. 1a), being either co-present or co-absent with *MICU1* in 495 of 500 organisms evaluated (Hamming distance = 5). *MCU* is also the second highest scoring gene in the genome-wide mRNA co-expression analysis (Fig. 1b) and is the top scoring protein amongst all ~1,100 mitochondrial proteins for protein coexpression with MICU1 across 14 mouse tissues (Fig. 1c).

Our prediction of a functional relationship between MICU1 and MCU was further corroborated by evidence of a physical interaction. By transfecting green-fluorescent-protein-tagged MCU (MCU–GFP) into cells stably expressing V5-tagged MICU1 (MICU1–V5) and vice versa, we were able to recover both GFP-tagged proteins following

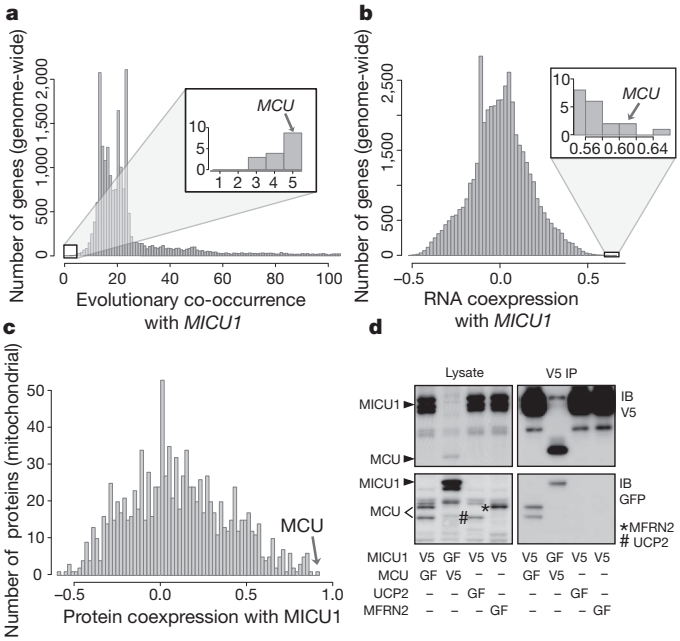

Figure 1 | Integrative genomics predicts MCU to be functionally related to MICU1 **a–c**, Phylogenetic profile neighbours (**a**), RNA co-expression neighbours (**b**) and protein co-expression neighbours (**c**) of MICU1. Hamming distances between phylogenetic profiles were computed genome-wide for all 20,000 mammalian genes across 500 fully sequenced organisms. Genes co-expressed with *MICU1* were computed genome-wide by Pearson correlation using a mouse atlas of 81 tissues. Protein expression correlation with MICU1 was analysed for all mitochondrial proteins across 14 mouse tissues. **d**, Coimmunoprecipitation of MICU1 and MCU. HEK-293 cells stably expressing MICU1–V5 or MCU–V5 were transfected with MICU1–GFP, MCU–GFP, MFRN2–GFP or UCP2–GFP. Cell lysates were incubated with anti-V5 antibody, immunoprecipitates were resolved on SDS–PAGE, and input lysates and immunoprecipitates were blotted with anti-V5 (top) or anti-GFP (bottom) antibodies. Data are representative of three independent experiments. IP, immunoprecipitation; GF, green fluorescent protein; IB, immunoblot.

[1]Departments of Systems Biology and Medicine, Harvard Medical School and Massachusetts General Hospital, Boston, Massachusetts 02114, USA. [2]Broad Institute, Cambridge, Massachusetts 02142, USA. [3]Koch Institute for Integrative Cancer Research, Massachusetts Institute of Technology, Cambridge, Massachusetts 02139, USA. [4]Alnylam Pharmaceuticals, Inc., Cambridge, Massachusetts 02142, USA.

*These authors contributed equally to this work.

immunoprecipitation with an anti-V5 antibody (Fig. 1d). The interaction was specific as MICU1–V5 was incapable of pulling down two different GFP-tagged inner membrane proteins (UCP2 and MFRN2, also known as SLC25A28). Similar results were also obtained by immunoprecipitating Flag-tagged MCU and probing for endogenous MICU1 (Supplementary Fig. 1).

Collectively, our three complementary genomic analyses combined with our biochemical data (Fig. 1) predict that MCU is functionally related to MICU1 and that it, too, may participate in mitochondrial Ca^{2+} uptake.

We evaluated the impact of silencing *MCU* on mitochondrial Ca^{2+} uptake in intact and permeabilized cells using RNA interference (RNAi). Silencing *MCU* in a HeLa cell line expressing a mitochondria-targeted aequorin (mt-Aeq) reporter[9] attenuates mitochondrial Ca^{2+} uptake (Fig. 2a) proportionate to the strength of knockdown (Fig. 2b). The RNAi-induced phenotype is not off-target because coexpression of a full-length *MCU* cDNA together with a short hairpin RNA (shRNA) that targets the *MCU* 3′ untranslated region (3′UTR) fully rescues Ca^{2+} uptake (Fig. 2a). Moreover, the RNAi effect is not a trivial consequence of interrupting upstream signalling, because histamine mobilization of cytosolic Ca^{2+} remains intact (Supplementary Fig. 2a), and because we obtain similar results when measuring clearance of exogenously added Ca^{2+} by mitochondria in permeabilized HEK-293 (Fig. 2c) and HeLa cells (Supplementary Fig. 3). In HeLa cells, basal and uncoupled respiration were intact (Supplementary Fig. 2b), mitochondrial membrane potential (ψ_m) was not depolarized (Supplementary Fig. 2c), and mitochondrial morphology remained grossly unchanged (data not shown) after silencing of *MCU*. Basal cytosolic Ca^{2+} levels were 53.9 nM ± 16.3 ($n = 30$) in *MCU* knockdown HeLa cells and 70.9 nM ± 11.7 ($n = 14$) in control sh-LACZ cells. Although mitochondrial Ca^{2+} buffering is known to shape cytosolic Ca^{2+} transients in many cell types, its inhibition through silencing of *MCU* did not show a significant impact on cytosolic Ca^{2+} clearance after histamine stimulation (Supplementary Fig. 2a). However, this result could reflect an incomplete silencing of *MCU*-mediated mitochondrial Ca^{2+} uptake in HeLa cells (Fig. 2a, b). Mitochondrial Ca^{2+} uptake has also previously been shown to stimulate ATP production by allosterically activating three tricarboxylic acid (TCA) cycle dehydrogenases[10]. Using a previously reported protocol[11], we found that permeabilized sh-MCU cells exhibit attenuated NAD(P)H elevation in response to exogenously added Ca^{2+} (Supplementary Fig. 2d), demonstrating that silencing *MCU*, like *MICU1* (ref. 5), attenuates Ca^{2+} activation of the TCA cycle.

To complement these cell-based studies, we analysed mitochondrial calcium uptake in mouse liver mitochondria upon *in vivo* silencing of *MCU*. A key advantage of this experimental system is that Ca^{2+} uptake phenotypes are directly attributable to mitochondria, and additional bioenergetic parameters, notably respiratory flux and ψ_m, can be carefully measured under classic respiratory state transitions[12]. As respiratory state transitions are dependent on TCA cycle metabolism, electron transport, H^+ pumping, ATP/ADP exchange, and transport of phosphate, such studies allow us to evaluate the specificity of MCU's role in mitochondrial Ca^{2+} transport. Using previously described siRNA design and delivery technology[13], we screened 46 distinct siRNA duplexes. We selected a duplex characterized by a half-maximal inhibitory concentration of 69 pM that achieved >90% knockdown at a concentration of 5 nM in cultured mouse liver cells (Fig. 2d). We performed a large-scale synthesis of this siRNA duplex and encapsulated it into a lipid-based formulation optimized for liver-specific delivery[14,15]. As a negative control we used a siRNA duplex specific for the firefly luciferase gene (si-LUC). We performed weekly tail vein injections of the siRNA duplexes over a 3 week period and achieved 84 ± 2% ($n = 3$) *in vivo* mRNA knockdown of *MCU* in the liver, which was corroborated by immunoblot analysis (Fig. 2d). Both groups of mice showed normal weight gain (5.6 ± 1.3% of body weight for si-LUC and 5.0 ± 3.0% of body weight for si-MCU, $n = 3$) and the gross appearance of the livers did not differ. Mitochondria isolated from

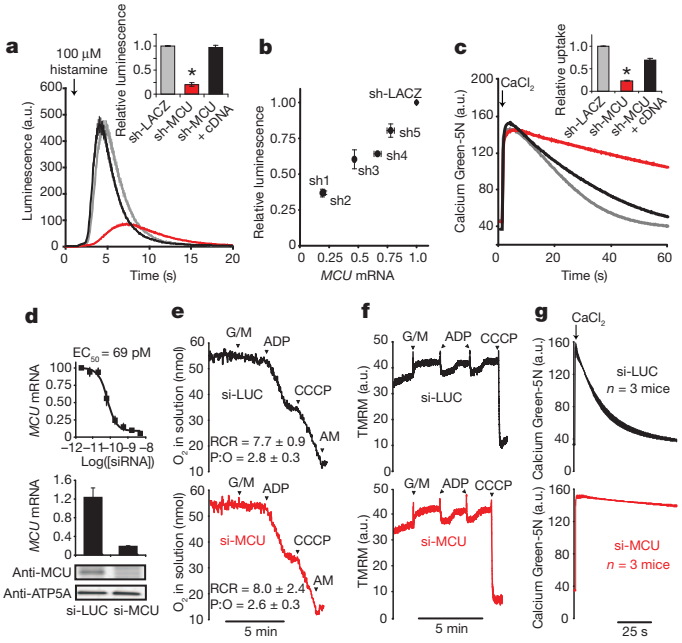

Figure 2 | MCU is required for mitochondrial Ca^{2+} uptake in cultured cells and in purified mouse liver mitochondria. **a**, Representative luminescence measurements of a mitochondrial aequorin Ca^{2+} reporter after histamine stimulation in HeLa cells expressing sh-LACZ, sh-MCU, or a combination of sh-MCU and an RNAi-resistant cDNA for *MCU* (mean ± s.e.m., $n = 10$ traces). Inset shows statistical analysis of the maximal luminescence (mean ± s.d., $n = 10$ traces, $^*P < 0.001$). a.u., arbitrary units. **b**, Relationship between *MCU* mRNA expression and histamine-induced mitochondrial Ca^{2+} uptake (maximal aequorin luminescence) recorded from five independent shRNAs targeting *MCU* and normalized to sh-LACZ (mean ± s.d., $n = 3$). **c**, Representative traces of Ca^{2+} uptake in digitonin-permeabilized sh-MCU HEK-293 cells or sh-LACZ control cells after addition of 50 μM final concentration of $CaCl_2$. Inset reports linear fits of uptake kinetics between 15 and 20 s, normalized to sh-LACZ (mean ± s.d., $n = 3$, $^*P < 0.001$). Ca^{2+} was measured with Calcium Green-5N. **d**, *In vitro* dose–response of a selected siRNA duplex targeting mouse *MCU*. Relative expression of *MCU* mRNA in livers following weekly injections of si-MCU or si-LUC for 3 weeks, normalized to expression in PBS-treated mice. Immunoblot analysis of liver mitochondria isolated from mice treated with si-MCU or control si-LUC using antibodies against MCU and ATP5A1 as a loading control. **e**, Oxygen consumption measurements of isolated mitochondria in a well-stirred cuvette. Glutamate and malate (G/M), ADP, uncoupler (carbonyl cyanide *m*-chlorophenyl hydrazone, CCCP), antimycin (AM) were added at indicated time points. Respiratory control ratio (RCR) and ADP:O ratio (P:O) were computed from three separate mice for each group. **f**, Mitochondrial membrane potential (ψ_m) measured by tetramethyl rhodamine methyl ester (TMRM) in isolated liver mitochondria. **g**, Ca^{2+} uptake kinetics in energized liver mitochondria following the addition of 50 μM final $CaCl_2$. Extra-mitochondrial Ca^{2+} was measured with Calcium Green-5N (mean ± s.e.m., $n = 3$ mice). Traces depicted in **e** and **f** are representative of measurements made from three independent mouse experiments performed on separate days.

these livers were physiologically intact, capable of undergoing robust respiratory state transitions (Fig. 2e, f). The respiratory control ratio (RCR) was comparable in si-LUC (7.7 ± 0.9, $n = 3$) and si-MCU animals (8.0 ± 2.4, $n = 3$). The ADP:O ratios were 2.77 ± 0.3 ($n = 3$) and 2.61 ± 0.3 ($n = 3$) in si-LUC and si-MCU mitochondria, respectively, indicating intact respiratory chain physiology. However, mitochondria from si-MCU mice show a profound and near complete loss in Ca^{2+} uptake in response to extramitochondrial pulses of Ca^{2+} (Fig. 2g and Supplementary Fig. 4).

Collectively, our physiology studies, comprising three different experimental systems (intact cells, permeabilized cells and mitochondria purified from mouse organs), three different cell types (HeLa, HEK-293 and mouse liver), and two different silencing modalities (*in vitro* lentiviral shRNA and *in vivo* siRNA), firmly establish that

MCU is essential for high capacity Ca^{2+} transport into mitochondria, and that the phenotype is not a secondary consequence of alterations in cytosolic Ca^{2+} signalling or of impaired ion or metabolite transport across the mitochondrial inner membrane. To our knowledge, this is the first time that mitochondrial Ca^{2+} uptake has been silenced *in vivo* in an animal.

We next established MCU's precise sub-organellar localization and topology. MCU was first identified as a mitochondrial protein in our previous proteomic survey[6], where it was detected as a low abundance protein in 12 out of 14 mouse tissues, being missed only in heart and kidney. Confirmatory immunoblot analysis suggests it is also present in the heart and the kidney (data not shown), indicating it is universally expressed. As expected, a carboxy terminus GFP-tagged version of MCU localizes exclusively to mitochondria in HeLa cells (Fig. 3a) as well as in HEK-293 cells (data not shown). To biochemically validate MCU's localization, we fractionated HeLa cell lysate and observed significant enrichment of the approximately 35 kDa native MCU in the mitochondrial fraction (Fig. 3b). The observed molecular weight of MCU is lower than the predicted 40 kDa and is consistent with a predicted cleavable amino-terminal mitochondrial targeting sequence[16]. Multiple algorithms predict that MCU contains two transmembrane domains[17,18]. To experimentally confirm mitochondrial inner-membrane integration and to discriminate between transmembrane and peripheral membrane configurations, we performed alkaline carbonate extraction of proteins from intact mitochondria isolated from HEK-293 cells expressing MCU-V5. We find that MCU remains in the insoluble fraction, proving that it is a bona fide transmembrane protein (Fig. 3c). To establish the topology of MCU across the inner membrane, we disrupted the mitochondrial outer membrane by hypotonic swelling and treated the resulting mitoplasts with proteinase K. Proteins such as OXA1 that are exposed to the mitochondrial intermembrane space are digested by proteinase K, whereas COII (an integral inner membrane protein, also known as MT-CO2) and MCU are completely protected (Fig. 3d), despite being substrates for proteinase K (Supplementary Fig. 5). Our data therefore indicate that MCU is localized to the inner membrane with both its N- and C-termini facing the matrix space.

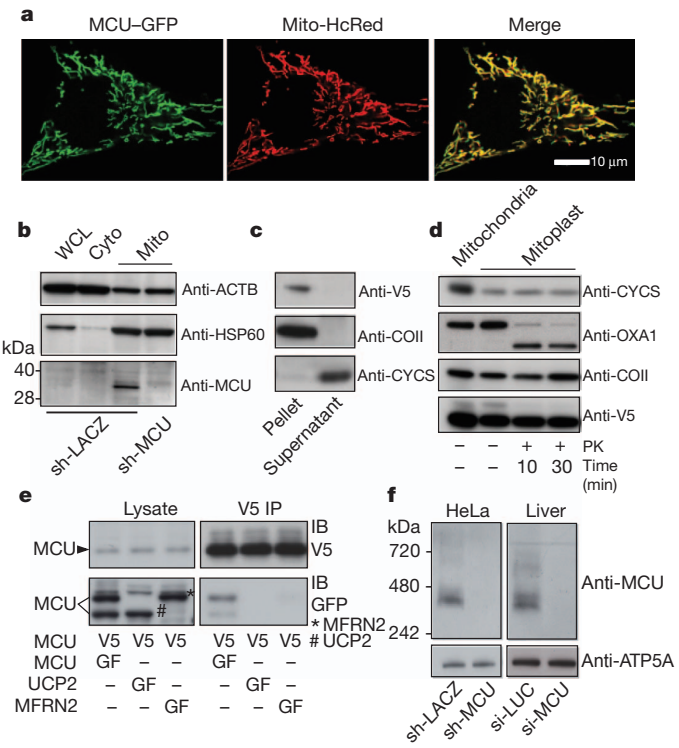

Figure 3 | MCU is oligomeric and resides in the mitochondrial inner membrane as a larger complex. **a**, Confocal imaging of MCU–GFP co-expressed with mitochondria-targeted HcRed (Mito-HcRed) in HeLa cells. **b**, Immunoblot analysis of HeLa whole-cell lysate (WCL), cytosol (Cyto) or crude mitochondrial fractions (Mito), using antibodies against MCU, HSP60 (matrix protein, also known as HSPD1), or ACTB (cytosol). **c**, Immunoblot analysis of soluble (supernatant) and insoluble (pellet) fractions following alkaline carbonate extraction of mitochondrial fractions from HEK-293 cells expressing MCU–V5. Immunoblot analysis was performed using antibodies against V5, COII (integral inner membrane protein) and CYCS (soluble intermembrane space protein). **d**, Immunoblot analysis after proteinase K (PK) treatment of MCU–V5-expressing HEK-293 mitoplasts for indicated times. **e**, Anti-V5 immunoprecipitations performed as in Fig. 1d using lysates from HEK-293 cells stably expressing MCU–V5 and transiently transfected with MCU–GFP, UCP2–GFP, or MFRN2–GFP. **f**, Blue native PAGE analysis of mitochondrial fractions from HeLa cells (stably expressing sh-LACZ or sh-MCU, left panel) or from livers of mice (si-LUC or si-MCU, right panel) and immunoblotted for MCU. ATP5A1 is used as a loading control.

If MCU is an integral component of the uniporter, we might expect that it oligomerizes and operates within a larger complex. To test for MCU oligomerization, we performed pull-down experiments and found that V5-tagged MCU is capable of immunoprecipitating GFP-tagged MCU (Fig. 3e), indicating that MCU can form multimers. To control for nonspecific interactions we used two inner mitochondrial membrane spanning transporters as controls, neither of which immunoprecipitated with MCU–V5 (Fig. 3e). We performed blue native gel separation of digitonin-solubilized mitochondria purified from HeLa cells and found that MCU migrates at an apparent molecular weight of ~450 kDa. This larger complex disappears following silencing with sh-MCU (Fig. 3f, left panel). We obtained similar results using mitochondria from livers of si-LUC and si-MCU mice (Fig. 3f, right panel). Collectively, these studies indicate that MCU oligomerizes in the mitochondrial inner membrane as part of a larger molecular weight complex.

Our topology analysis (Fig. 3c, d) combined with computational predictions of membrane spanning domains indicate that MCU's two transmembrane helices, TM1 and TM2, are linked by a short stretch of amino acids that face the intermembrane space and contain what we now term a 'DIME' motif (Fig. 4a). We sought to determine whether conserved amino acids near and within the DIME motif are required for MCU-mediated Ca^{2+} uptake. We created a series of four alanine mutants at conserved residues (E257A, S259A, D261A, E264A) and expressed them on an sh-MCU background to evaluate their ability to rescue Ca^{2+} transport (Fig. 4b). One mutant, S259A, was capable of providing significant rescue of the sh-MCU phenotype (Fig. 4b). The remaining three mutants (E257A, D261A, E264A), however, failed to restore mitochondrial calcium uptake despite comparable expression to the S259A mutant (Supplementary Fig. 6a), signifying that these highly conserved acidic residues are critical for Ca^{2+} transport.

Ruthenium red and a related compound, Ru360, are the most potent inhibitors of the mitochondrial Ca^{2+} uniporter, yet their target remains unknown[19,20]. These cell-impermeant inhibitors have been useful pharmacological tools in studies of isolated mitochondria[21,22] and are believed to act on the outer face of the inner membrane. We next sought to determine whether the functional S259A mutant might influence Ru360 sensitivity. Ru360 strongly abolishes mitochondrial Ca^{2+} uptake in permeabilized HEK-293 cells (Fig. 4c). Transient overexpression of *MCU* leads to a mild resistance to Ru360 compared to control (Fig. 4c). However, transient expression of the S259A mutant confers marked resistance to Ru360 in both HEK-293 and HeLa cells (Fig. 4c, Supplementary Fig. 6b, c, d, e). These experiments clearly indicate a functional role for the linker region in both activity and Ru360 sensitivity of MCU.

Our genomic, physiological, biochemical and pharmacological data firmly establish that MCU is an oligomeric, mitochondrial inner membrane protein that is essential for calcium uniporter activity. In our current studies, overexpression of *MCU* alone did not give rise to a

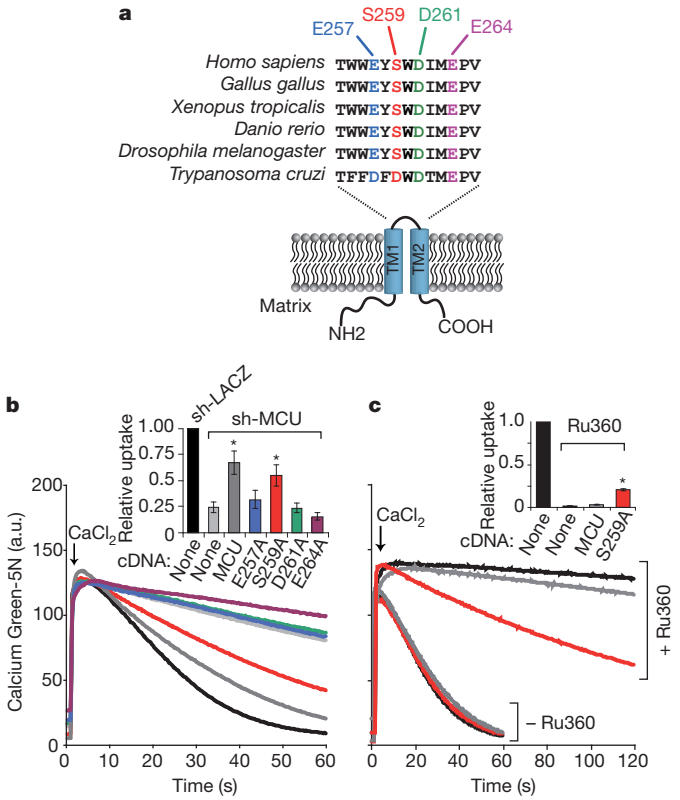

Figure 4 | Impact of point mutations on MCU activity and its sensitivity to Ru360. **a**, Schematic of MCU topology across the mitochondrial inner membrane and a multiple sequence alignment of the linker sequence containing a DIME motif. TM1 and TM2 are two transmembrane domains. **b**, Ca^{2+} uptake in permeabilized sh-MCU HEK-293 cells transiently expressing MCU mutants. Inset reports linear fits of uptake kinetics between 15 and 25 s, normalized to sh-LACZ (mean ± s.d., $n = 3$, $^*P < 0.01$) **c**, Ca^{2+} uptake in HEK-293 cells transiently expressing wild-type MCU or the S259A mutant, in the presence or absence of 0.5 μM Ru360. Inset reports linear fits of uptake kinetics between 30 and 60 s for Ru360-treated cells, and between 15 and 25 s for untreated cells. Uptake rates are normalized to untreated HEK-293 cells (mean ± s.d., $n = 3$, $^*P < 0.01$).

marked gain of Ca^{2+} uptake in HeLa cells (Fig. 2a), indicating that additional components or chaperones may be limiting *in vivo*. Although its precise mechanism remains to be elucidated, MCU fulfils multiple criteria for being an integral component of the uniporter, where it could serve as the pore-forming subunit or as a closely associated partner protein. First, loss of *MCU* leads to a profound defect in mitochondrial Ca^{2+} uptake in three distinct systems: intact cells, permeabilized cells and mouse liver (Fig. 2). Second, it has two bona fide transmembrane domains and oligomerizes to form a larger molecular weight complex in the mitochondrial inner membrane (Fig. 3e, f). Third, mutations at evolutionarily conserved acidic residues attenuate its activity (Fig. 4b). Fourth, a point mutation in MCU confers resistance against Ru360, the most potent inhibitor of the uniporter (Fig. 4c and Supplementary Fig. 6). The current study further supports our previously reported phylogenomic signature of the mitochondrial Ca^{2+} uniporter[5], and together these studies identify MICU1 and MCU as an evolutionarily conserved duo that are critical for mitochondrial Ca^{2+} uptake. Whereas MICU1 may serve as a regulator, MCU is likely to represent a core component of the uniporter. Future studies will be necessary to establish the exact mechanism by which these proteins function together to orchestrate the mitochondrial Ca^{2+} cycle.

METHODS SUMMARY

Candidate human genes required for mitochondrial Ca^{2+} uptake were prioritized on the basis of the co-occurrence of their homologues with *MICU1* across 500 evolutionarily diverse organisms[6,7] and their RNA and protein co-expression across mouse cell types and tissues[6,8]. Stable knockdown of *MCU* in HeLa and HEK-293 cells was achieved using lentiviral shRNA-expressing constructs available from the Broad Institute RNAi Consortium[23]. *In vivo* silencing of *MCU* in mouse liver was achieved via weekly tail vein injections of selected siRNAs in lipid-based formulations[13–15,24]. cDNA rescue studies in *MCU* knockdown cells were carried out by overexpression of wild-type or mutant versions of full-length MCU cDNAs together with a shRNA that targets the *MCU* 3′UTR. Agonist-induced rises in mitochondrial Ca^{2+} in intact HeLa cells were measured by luminescence of a mitochondria-targeted aequorin reporter[9]. Extra-mitochondrial calcium in permeabilized HeLa cells, HEK-293 and isolated liver mitochondria was measured using Calcium Green-5N (ref. 5). Single-cell studies of cytosolic calcium were performed as previously described[25]. Mitochondrial respiration, membrane potential and NAD(P)H were measured via established protocols[11,26]. Crude mitochondria and mitoplasts were prepared from cultured HEK-293 cells expressing a C terminus V5-tagged version of MCU[5]. Protein topology was assessed by alkaline carbonate extraction from crude mitochondria and proteinase K digestion of mitoplasts[27]. Protein interaction studies were performed by immunoprecipitation with anti-V5 and anti-Flag antibodies. Native gel electrophoresis was performed as previously described[28]. Unless otherwise indicated, data are summarized as mean ± standard deviation (s.d.), and *P*-values were computed from *t*-tests.

Full Methods and any associated references are available in the online version of the paper at www.nature.com/nature.

Received 9 November 2010; accepted 2 June 2011.
Published online 19 June 2011.

1. DeLuca, H. F. & Engstrom, G. W. Calcium uptake by rat kidney mitochondria. *Proc. Natl Acad. Sci. USA* **47,** 1744–1750 (1961).
2. Vasington, F. D. & Murphy, J. V. Ca^{++} ion uptake by rat kidney mitochondria and its dependence on respiration and phosphorylation. *J. Biol. Chem.* **237,** 2670–2677 (1962).
3. Carafoli, E. & Lehninger, A. L. A survey of the interaction of calcium ions with mitochondria from different tissues and species. *Biochem. J.* **122,** 681–690 (1971).
4. Gunter, K. & Gunter, T. E. Transport of calcium by mitochondria. *J. Bioenerg. Biomembr.* **26,** 471–485 (1994).
5. Perocchi, F. *et al. MICU1* encodes a mitochondrial EF hand protein required for Ca^{2+} uptake. *Nature* **467,** 291–296 (2010).
6. Pagliarini, D. J. *et al.* A mitochondrial protein compendium elucidates complex I disease biology. *Cell* **134,** 112–123 (2008).
7. Pellegrini, M., Marcotte, E. M., Thompson, M. J., Eisenberg, D. & Yeates, T. O. Assigning protein functions by comparative genome analysis: protein phylogenetic profiles. *Proc. Natl Acad. Sci. USA* **96,** 4285–4288 (1999).
8. Lattin, J. E. *et al.* Expression analysis of G Protein-Coupled Receptors in mouse macrophages. *Immunome Res.* **4,** 5 (2008).
9. Rizzuto, R., Simpson, A. W., Brini, M. & Pozzan, T. Rapid changes of mitochondrial Ca^{2+} revealed by specifically targeted recombinant aequorin. *Nature* **358,** 325–327 (1992).
10. Denton, R. M. & McCormack, J. G. The role of calcium in the regulation of mitochondrial metabolism. *Biochem. Soc. Trans.* **8,** 266–268 (1980).
11. Territo, P. R., Mootha, V. K., French, S. A. & Balaban, R. S. Ca^{2+} activation of heart mitochondrial oxidative phosphorylation: role of the F_0/F_1-ATPase. *Am. J. Physiol. Cell Physiol.* **278,** C423–C435 (2000).
12. Chance, B. & Williams, G. R. Respiratory enzymes in oxidative phosphorylation. I. Kinetics of oxygen utilization. *J. Biol. Chem.* **217,** 383–393 (1955).
13. Musunuru, K. *et al.* From noncoding variant to phenotype via *SORT1* at the 1p13 cholesterol locus. *Nature* **466,** 714–719 (2010).
14. Akinc, A. *et al.* A combinatorial library of lipid-like materials for delivery of RNAi therapeutics. *Nature Biotechnol.* **26,** 561–569 (2008).
15. Akinc, A. *et al.* Targeted delivery of RNAi therapeutics with endogenous and exogenous ligand-based mechanisms. *Mol. Ther.* **18,** 1357–1364 (2010).
16. Claros, M. G. & Vincens, P. Computational method to predict mitochondrially imported proteins and their targeting sequences. *Eur. J. Biochem.* **241,** 779–786 (1996).
17. Bernsel, A., Viklund, H., Hennerdal, A. & Elofsson, A. TOPCONS: consensus prediction of membrane protein topology. *Nucleic Acids Res.* **37,** W465–W468 (2009).
18. Krogh, A., Larsson, B., von Heijne, G. & Sonnhammer, E. L. Predicting transmembrane protein topology with a hidden Markov model: application to complete genomes. *J. Mol. Biol.* **305,** 567–580 (2001).
19. Moore, C. L. Specific inhibition of mitochondrial Ca^{++} transport by ruthenium red. *Biochem. Biophys. Res. Commun.* **42,** 298–305 (1971).
20. Ying, W. L., Emerson, J., Clarke, M. J. & Sanadi, D. R. Inhibition of mitochondrial calcium ion transport by an oxo-bridged dinuclear ruthenium ammine complex. *Biochemistry* **30,** 4949–4952 (1991).
21. Bernardi, P. Mitochondrial transport of cations: channels, exchangers, and permeability transition. *Physiol. Rev.* **79,** 1127–1155 (1999).
22. Kirichok, Y., Krapivinsky, G. & Clapham, D. E. The mitochondrial calcium uniporter is a highly selective ion channel. *Nature* **427,** 360–364 (2004).

23. Moffat, J. *et al.* A lentiviral RNAi library for human and mouse genes applied to an arrayed viral high-content screen. *Cell* **124,** 1283–1298 (2006).
24. Semple, S. C. *et al.* Rational design of cationic lipids for siRNA delivery. *Nature Biotechnol.* **28,** 172–176 (2010).
25. Rebres, R. A. *et al.* Synergistic Ca^{2+} responses by $G\alpha_i$- and $G\alpha_q$-coupled G-protein-coupled receptors require a single PLCβ isoform that is sensitive to both $G\beta\gamma$ and $G\alpha_q$. *J. Biol. Chem.* **286,** 942–951 (2011).
26. Gohil, V. M. *et al.* Nutrient-sensitized screening for drugs that shift energy metabolism from mitochondrial respiration to glycolysis. *Nature Biotechnol.* **28,** 249–255 (2010).
27. Ryan, M. T., Voos, W. & Pfanner, N. Assaying protein import into mitochondria. *Methods Cell Biol.* **65,** 189–215 (2001).
28. Schagger, H. & von Jagow, G. Blue native electrophoresis for isolation of membrane protein complexes in enzymatically active form. *Anal. Biochem.* **199,** 223–231 (1991).

Supplementary Information is linked to the online version of the paper at www.nature.com/nature.

Acknowledgements We thank R. Nilsson, J. Engreitz and S. Calvo for bioinformatics assistance; D. Root and S. Silver for assistance in lentiviral RNAi; B. R. Bettencourt, K. Charisse, S. Kuchimanchi and L. Speciner for siRNA design, synthesis and formulation; M. Blower, J. Avruch and R. Ward for advice; and members of the Mootha laboratory for valuable feedback. J.M.B. and L.S. were supported by graduate student fellowships from the National Science Foundation. This work was supported by grants from the National Institutes of Health (GM0077465, DK080261) awarded to V.K.M.

Author Contributions J.M.B., F.P. and V.K.M. conceived of the project and its design. J.M.B., F.P., H.S.G., M.P., O.G., L.S., C.A.B.-T., X.R.B., Y.S. and R.L.B. performed experiments and data analysis. V.K. aided in experimental design. V.K.M., J.M.B., F.P. and M.P. wrote the manuscript.

Author Information Reprints and permissions information is available at www.nature.com/reprints. The authors declare no competing financial interests. Readers are welcome to comment on the online version of this article at www.nature.com/nature. Correspondence and requests for materials should be addressed to V.K.M. (vamsi@hms.harvard.edu).

METHODS

Phylogenetic profiling and co-expression analyses. We performed genome-wide phylogenetic profiling using a previously reported phylogenetic matrix across 500 sequenced genomes using the Hamming distance as our similarity metric[6]. For genome-wide mRNA co-expression analysis, we used a publicly available genome-wide tissue gene expression atlas (NCBI GSE10246)[8]. We used the published gene expression intensities normalized to the median for each chip, and then computed the Pearson correlation to *MICU1* expression. For protein co-expression analysis, we used our MitoCarta protein atlas of mitochondrial protein expression across 14 tissues[6]. We summarized the abundance of a protein as the number of detected peptides per protein per tissue, and computed the Pearson correlation to MICU1 expression.

Cell culture. HEK-293 cells, Hepa-1c1c7 and HeLa cells were received from the ATCC. HeLa cells expressing a mitochondrial matrix targeted aequorin (mt-Aeq) were purchased from Aequotech (AT-002-H). All cells were grown in Dulbecco's modified Eagle medium (DMEM) high glucose medium (Invitrogen) with 10% FBS (Sigma) at 37 °C and 5% CO_2. mt-Aeq cells were maintained in 100 μg ml^{-1} geneticin (Gibco).

Plasmids and reagents. Lentiviral vectors for expressing shRNA (pLKO.1) or V5-tagged cDNAs (pLEX983) were obtained from the Broad Institute's RNAi Consortium (TRC). To silence *MCU*, we used the following hairpins from the TRC: sh1 (TRCN0000137529, 5′-CCAGCAACTATACACCACACT-3′), sh2 (TRCN0000133861, 5′-GCAAGGAGTTTCTTTCTCTTT-3′), sh3 (TRCN0000133984, 5′-CAATCAACTCAAGGATGCAAT-3′), sh4 (TRCN0000135430, 5′-GCCATG GCAATGTATGCATAT-3′), sh5 (TRCN0000138929, 5′-GATCGCTTCCTGG CAGAATTT-3′). For transfections, cDNAs were inserted into pcDNA vectors with C-terminal V5/His6× or GFP tags (Invitrogen pDEST40 and pDEST47, respectively) using Gateway LR (Invitrogen). A full-length *MCU* human cDNA (NM_138357.1) without a stop codon was cloned into the pDONR223 Gateway vector and subsequently cloned into pLEX983, pDEST40 and pDEST47 vectors. MCU mutants E257A, S259A, D261A and E264A mutations were created using Stratagene QuikChange mutagenesis. We used TaqMan assays (ABI) to quantify the *MCU* transcript (*CCDC109A*).

Lentivirus production and infection. Procedures and reagents for virus production and infection were adapted from the Broad RNAi Consortium protocols and were described previously[23]. Selection was begun 24 h post-infection with 2 μg ml^{-1} puromycin or 5 μg ml^{-1} blasticidin.

Rescue of sh-*MCU* and overexpression of MCU mutants. HeLa cells stably overexpressing shRNAs targeting either *LACZ* or the 3′UTR of *MCU* (TRCN0000133861) were transduced with either pLEX983-MCU wild-type or mutant versions and selected with 5 μg ml^{-1} blasticidin for at least 1 week before assaying. Wild-type HEK-293 or HEK-293 cells stably overexpressing sh-MCU (TRCN0000133861) were transfected with wild-type or mutant MCU cDNAs using Fugene6 reagent from Roche. To ensure high transfection efficiency HEK-293 were transfected twice 3 days apart and Ca^{2+} uptake was assayed 7 days after the first transfection.

Synthesis and *in vitro* screening of siRNAs targeting *MCU*. siRNAs with the lowest predicted off-target potentials (46) and 100% homology with mouse sequence NM_001033259.3 were selected for synthesis and screening. Single-strand RNAs were produced at Alnylam Pharmaceuticals as previously described[13]. MCU siRNA duplex with lowest EC_{50} and lowest predicted off-target potential was selected. The siRNA sense strand is 5′-GAcuGAGAGA cccAuuAcAdTsdT-3′, antisense is 5′-UGuAAUGGGUCUCUcAGUCdTsdT-3′; control luciferase siRNA sense is 5′-cuuAcGcuGAGuAcuucGAdTsdT-3′, and antisense is 5′-UCGAAGuACUcAGCGuAAGdTsdT-3′. Chemical modifications were introduced to stabilize siRNA *in vivo*, reduce off-target potential of sense strand and minimize immune response (2′-OMe modified nucleotides are in lower case, and phosphorothioate linkages are indicated by 's'). Hepa-1c1c7 cells (seeded 15,000 cells per well in 96-well plates) were transfected with siRNA using the Lipofectamine RNAiMAX reagent according to the manufacturer's protocols. *MCU* mRNA levels were quantified in cell lysates 18–24 h post-transfection using a branched-DNA assay (QuantiGene Reagent System, Panomics), according to the manufacturer's protocols. *MCU* mRNA levels were normalized to *GAPDH* mRNA.

***In vivo* silencing of *MCU*.** All procedures used in animal studies were approved by the Institutional Animal Care and Use Committee. C57BL/6 mice (Charles River laboratories) received either PBS or siRNA in lipid-based formulations (as previously described[14,15,24]) via tail vein injection weekly. After overnight fasting the animals were euthanized by CO_2 inhalation and liver tissues were collected into ice-cold PBS for mitochondria isolation. A piece of liver tissue was snap-frozen in liquid nitrogen for measurements of mRNA and protein levels.

Luminescence-based measurement of mitochondrial Ca^{2+}. Assays were performed using either mt-Aeq HeLa cells that stably express mitochondrial aequorin (Fig. 2b) or wild-type HeLa cells that were transduced with an equal titre of lentivirus to express mitochondrial-targeted aequorin[9] 3 days before assaying (Fig. 2a). 12–18 h before assaying, 50,000 cells were seeded per well in a 96-well plate. Light emission after histamine stimulation was measured as reported previously[5]. After histamine stimulation, cells were treated with 1% Triton X-100 and 10 mM $CaCl_2$ (final concentrations) and the light emission was recorded. To normalize, the maximal luminescence signal after histamine stimulation was divided by the total luminescence recorded per well in the entire experiment.

Measurements of cytosolic Ca^{2+}. Calibrated measurements of cytosolic Ca^{2+} were made via single-cell imaging of cells loaded with 500 nM Fura-2, calibrated as previously described[25]. Population measurement of cytosolic Ca^{2+} in response to 100 μM histamine was performed essentially as described in the Alliance for Cell Signalling protocols (PP00000210) except for using 4 μM Fluo-4 AM-ester and 200,000 cells per well in suspension. Minimum calibration was achieved with 5 μM ionomycin and 5 mM EGTA. Maximum calibration was achieved with 1% Triton X-100 and 20 mM $CaCl_2$ final concentrations. The K_d of Fluo-4 was assumed to be 350 nM.

Assays of ψ_m, oxygen consumption and NAD(P)H in intact and permeabilized cells. For measurements of membrane potential, HeLa cells (50,000 per treatment) were seeded in eight wells of a 96-well plate and incubated with 3.5 μM JC-1 for 20 min. The uncoupler CCCP (5 μM) was added as a positive control. The wells were washed at least four times with phenol-red-free DMEM before measuring. For assaying, red fluorescence (excitation 531 nm, emission 590 nm) was measured followed by green fluorescence (excitation 488 nm, emission 535 nm) in a Perkin-Elmer Envision fluorescence plate reader. Background fluorescence values recorded from wells without cells were subtracted from all fluorescence values before calculating red/green fluorescence ratios. Intact cell respiration was measured using Seahorse XF-24 Extracellular Flux Analyzer, as previously described[26]. To investigate Ca^{2+} stimulation of mitochondrial NAD(P)H in permeabilized HEK-293 cells, we adapted a previously described protocol[11].

Measurement of mitochondrial Ca^{2+} uptake in permeabilized cells. Extramitochondrial free Ca^{2+} was monitored in digitonin-permeabilized cells as previously described[5]. Calcium Green-5N fluorescence (excitation 506 nm, emission 531 nm) was monitored every 0.2 s at room temperature using a Perkin-Elmer Envision plate reader after injection of $CaCl_2$ (~50 μM final concentration). For Ru360 (Calbiochem #557440) treatments, selected concentrations of Ru360 or H_2O (vehicle) were added to the digitonized cells and incubated 2 min before $CaCl_2$ injection. For calculation of relative Ca^{2+} uptake, linear fits were computed for the times indicated.

Mitochondrial isolation, mitoplast preparation, and topology analysis. Cell lysates, crude mitochondria and mitoplasts were prepared from cultured HEK-293 cells as previously described[5]. Immunoblotting of the four fractions (5 μg) was performed with commercially available antibodies: anti-MCU (Sigma #HPA016480), anti-HSP60 (Abcam ab3080), anti-CYCS (MitoSciences #MSA06), anti-OXA1 (BD Biosciences #611980), anti-COII (MitoSciences #MS405) and anti-V5 (Invitrogen, R96025). Alkaline carbonate extraction from crude mitochondria and proteinase K digestion of mitoplasts were performed as described previously[27].

Measurement of respiration, ψ_m and Ca^{2+} uptake in isolated mouse mitochondria. Mitochondria were isolated from freshly collected mouse livers as previously described[26] and resuspended into a buffer containing 220 mM mannitol, 75 mM sucrose, 10 mM HEPES-KOH pH 7.4, 1 mM EDTA and 0.5% BSA and stored on ice until further use. Respiration and ψ_m were measured optically in a well-stirred cuvette as previously described[26]. For Ca^{2+} uptake measurements, 400 μg of isolated mitochondria were resuspended in 500 μl of potassium chloride (KCl) media (125 mM KCl, 2 mM K_2HPO_4, 1 mM $MgCl_2$, 20 mM HEPES-KOH pH 7.4) containing 1 μM Calcium Green-5N and 5 mM glutamate and 5 mM malate. Fluorescence was monitored at room temperature using a Perkin-Elmer LS-50B fluorescence spectrometer equipped with a stirring device. Respiratory control ratios (RCRs) were computed as the ratio of the ADP-stimulated respiration to the respiratory substrates-based respiration. The ADP:O ratio was computed after correcting for the oxygen leak into the cuvette. Values represent the mean ± s.d. of three, independent biological replicate mouse injections performed on three different days.

Confocal microscopy. HeLa cells cultured in Lab-Tek II chambered slides were co-transfected with plasmids expressing MCU–GFP and Mito-HcRed (Clontech #632434). Twenty-four hours post-transfection, cells were washed three times with PBS and imaged using a Leica TCS SP5 confocal microscope.

Blue native studies. Membrane protein complexes were separated by electrophoresis as previously described[28]. Briefly, mitochondria were isolated from ~20 million HeLa cells stably expressing sh-LACZ or sh-MCU according to the MitoSciences protocol (catalogue no. MS851). Total protein was quantified by bicinchoninic assay and 5 μg of mitochondria were solubilized in 1% digitonin

(w/v) on ice. Electrophoresis was performed using the NativePAGE Novex Bis-Tris Gel System from Invitrogen. Protein was transferred to a polyvinylidene fluoride (PVDF) membrane and immunoblotted with a commercially available antibody to MCU (Sigma #HPA016480). Membranes were stripped and re-probed with anti-ATP5A1 (MitoSciences MS507) as a loading control.

Immunoprecipitation studies. One confluent 10-cm dish of HEK-293 cells stably overexpressing either MICU1–V5 or MCU–V5 was washed twice with ice-cold PBS approximately 36 h post-transfection with either MCU–GFP or MICU1–GFP. Cells were lysed for 30 min with 1 ml of lysis buffer containing 1% *n*-dodecyl β-D-maltoside (DDM), 150 mM NaCl, and 50 mM Tris pH 7.4, and the insoluble fraction was removed by centrifugation. The soluble fraction was incubated with Dynabeads Protein G (Invitrogen 100-04D) coated with anti-V5 antibody (Invitrogen #R960-25). Immunoprecipitations were performed according to the manufacturer's guidelines. Eluents were immunoblotted with anti-V5 antibody to confirm binding and with anti-GFP antibody to probe for interactions (Novus catalogue number NB600-308). For anti-Flag immunoprecipitation studies in Supplementary Fig. 1, 2 million HEK-293 cells were plated in 10-cm plates. Cells were transfected with 2 μg of indicated plasmids using Fugene6 1 day later. After 2 days, cells were solubilized in 1 ml of lysis buffer (50 mM HEPES KOH, pH 7.4, 10 mM sodium pyrophosphate, 2 mM EDTA, 1% Triton X-100), centrifuged for 10 min at 15,000*g* and cleared lysates were incubated with anti-Flag M2 affinity gel (Sigma A2220) for 2 h at 4 °C. The immunoprecipitates were washed once with 1 ml of lysis buffer and three times with lysis buffer including 200 mM NaCl. After the last wash, the immunoprecipitates were boiled in 40 μl of SDS sample buffer. The immunoprecipitates (15 μl) were used for immunodetection using anti-Flag (Sigma F1804) and anti-MICU1 (Abcam).